

Heavy leptons from W decay

V. Barger and H. Baer

Physics Department, University of Wisconsin, Madison, Wisconsin 53706

A. D. Martin and E. W. N. Glover

Physics Department, University of Durham, Durham, England

R. J. N. Phillips

Rutherford Appleton Laboratory, Chilton, Didcot, Oxon, England

(Received 18 November 1983)

We investigate the possibility of detecting a new heavy lepton at the $\bar{p}p$ collider through the decay mode $W \rightarrow L\nu_L$. We consider both the leptonic ($L \rightarrow e\nu_e\bar{\nu}_L$) and hadronic ($L \rightarrow \bar{q}Q\bar{\nu}_L$) sequential decays of the L . We present detailed calculations to show that the leptonic decay rate is exceeded, for all kinematic ranges, by background contributions from $W \rightarrow e\nu_e$ and $W \rightarrow \tau\nu_\tau \rightarrow e\nu_e\bar{\nu}_\tau\nu_\tau$ decays. On the other hand, the hadronic decay leads to a promising, distinctive signature: a large missing transverse momentum balanced by two recognizable jets. Selective cuts can be imposed to remove background contributions, and the remaining event rate is about 10% of the $W \rightarrow e\nu$ rate if the mass of the lepton is below 50 GeV.

I. INTRODUCTION

One of the crucial questions of particle physics is whether or not there are more than three generations of quarks and leptons. For example, does the sequence (e, ν_e) , (μ, ν_μ) , (τ, ν_τ) continue to a fourth weak-isospin doublet (L, ν_L) ? Experiments¹ at e^+e^- colliders require the mass of such a new lepton L to be greater than 20 GeV.

The discovery of W^\pm bosons² at the CERN $\bar{p}p$ collider offers the realistic possibility of searching for a new sequential heavy lepton L , with mass less than M_W , via the decay $W \rightarrow L\bar{\nu}_L$ with the subsequent leptonic or hadronic decay of the L ; that is

$$L \rightarrow e\bar{\nu}_e\nu_L, \mu\bar{\nu}_\mu\nu_L, \quad (1)$$

$$L \rightarrow d\bar{u}\nu_L, s\bar{c}\nu_L, \quad (2)$$

respectively.

We see, however, that the leptonic decay chain

$$W \rightarrow L\bar{\nu}_L \rightarrow e\bar{\nu}_e\nu_L\bar{\nu}_L \quad (3)$$

has the same signature as the direct and the τ -initiated decay modes of the W ,

$$W \rightarrow e\bar{\nu}_e, \quad (4)$$

$$W \rightarrow \tau\bar{\nu}_\tau \rightarrow e\bar{\nu}_e\nu_\tau\bar{\nu}_\tau, \quad (5)$$

namely, an isolated energetic electron accompanied by missing transverse momentum (arising from the neutrinos). We devote Sec. II to a quantitative study of the properties of the electron spectrum from the leptonic decays of W bosons, with careful considerations of the background that were not addressed in a previous study.³

In Sec. III we consider ways of optimizing the L leptonic decay signal, Eq. (3), with respect to the back-

ground. Besides processes (4) and (5), we investigate the background arising from heavy-quark production in which one of the quarks decays semileptonically, for example,

$$\bar{p}p \rightarrow \bar{b}bX \text{ with } b \rightarrow ce\bar{\nu}_e. \quad (6)$$

We find that the L leptonic decay signal could be plagued by serious backgrounds of this type as well as those in Eqs. (4) and (5). We discuss possible lepton-isolation cuts to suppress the $b\bar{b}$ background.

In Sec. IV, we turn to the hadronic-decay signature of the L :

$$W \rightarrow L\bar{\nu}_L \rightarrow Q\bar{q}\nu_L\bar{\nu}_L. \quad (7)$$

Taking color into account, we expect the total hadronic decay rate to be 6 times that of a leptonic decay rate. Since there is an energetic primary neutrino ($\bar{\nu}_L$) and only one secondary neutrino (ν_L), we expect these events to be characterized by high missing transverse momentum balanced by two hadronic jets. Again we critically investigate possible background contributions and propose ways of optimizing the L signal. We find that the background can be effectively eliminated and conclude that the hadronic decay mode offers a distinctive practical signature for a new heavy lepton.

The experimental signatures of heavy leptons from W decay are similar to those associated with the W decay into gauge fermions in supersymmetric theories. In a wide class of supersymmetric theories there is the possibility of the decay chains⁴

$$W \rightarrow \tilde{W}\tilde{\gamma} \rightarrow e\nu_e\tilde{\gamma}\tilde{\gamma}, \quad (8)$$

$$W \rightarrow \tilde{W}\tilde{\gamma} \rightarrow Q\bar{q}\tilde{\gamma}\tilde{\gamma}, \quad (9)$$

where the \tilde{W} and the photino $\tilde{\gamma}$ are the supersymmetric

spin- $\frac{1}{2}$ partners of the W and γ , respectively. Although we do not explicitly discuss supersymmetric modes, our general considerations with minor modifications will apply equally to these W decay possibilities.

An abbreviated account of some of these results was presented in Ref. 5.

II. LEPTONIC DECAYS OF W BOSONS

Here we present the electron distributions resulting from W decays. The W partial widths for the leptonic decay modes (3)–(5) are taken to be in the ratio

$$(W \rightarrow e):(W \rightarrow \tau \rightarrow e):(W \rightarrow L \rightarrow e) = 1:0.17:\frac{1}{9}(1 - \frac{3}{2}r + \frac{1}{2}r^3) \quad (10)$$

with $r = m_L^2/M_W^2$. The estimate of the $W \rightarrow L \rightarrow e$ branching ratio takes account of the $d\bar{u}\nu_L$, $s\bar{c}\nu_L$, and the three primary leptonic decay channels of the L . We ignore decay chains such as $W \rightarrow L \rightarrow \tau \rightarrow e$ and $W \rightarrow L \rightarrow c \rightarrow e$, which are smaller contributions and which give very soft electrons. Although we frame the discussion in terms of decay electrons, the results apply equally well to muons. Indeed, since we will be emphasizing transverse momenta of around 10 GeV, the observation of muons may be preferred from an experimental viewpoint.

To be specific let us calculate the e^+ spectrum for $\bar{p}p \rightarrow WX \rightarrow e^+X$ resulting from the three decay modes of the W . We use the quark structure functions of Ref. 6 evolved in Q^2 up to $Q^2 = \hat{s}$, where $\sqrt{\hat{s}}$ is the center-of-

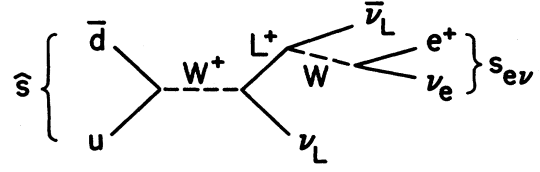


FIG. 1. The production and leptonic decay of an L^+ heavy lepton.

mass energy of the annihilating \bar{d} and u quarks; we repeated the analysis using the structure functions of Ref. 7 and found essentially identical results. We include u , d , s , and c sea-quark contributions in the nucleon, assuming an SU(4)-symmetric sea. This gives the most conservative estimate for the $W \rightarrow e\nu$ background. In fact there is little difference in the predictions of an SU(2)-symmetric u, d sea and the SU(4) case, except for the height of a sharp peak at backward angles (i.e., with the e^+ antiparallel to the \bar{p} direction). We calculate all distributions and cross sections in this paper using Monte Carlo techniques. Typically we use 10^5 shots, which corresponds to a numerical uncertainty of about 5% in the predictions.

The amplitude for the sequential decay process of Fig. 1

$$\bar{d}u \rightarrow W^+ \rightarrow L^+ \nu_L \rightarrow e^+ \nu_e \bar{\nu}_L \quad (11a)$$

is of the form

$$\begin{aligned} \mathcal{M} = & \left[\frac{G_F}{\sqrt{2}} \right]^2 \frac{M_W^2}{\hat{s} - M_W^2 + iM_W\Gamma_W} [\bar{v}(d)\gamma^\mu(1-\gamma^5)u(u)][\bar{u}(\nu_e)\gamma^\nu(1-\gamma^5)v(e)] \\ & \times \left[\bar{u}(\nu_L)\gamma_\mu(1-\gamma^5) \frac{P_L + m_L}{P_L^2 - m_L^2 + im_L\Gamma_L} \gamma_\nu(1-\gamma^5)v(\nu_L) \right] \left[\frac{M_W^2}{s_{e\nu} - M_W^2} \right], \end{aligned} \quad (11b)$$

where \hat{s} and $s_{e\nu}$ are shown in Fig. 1. Squaring and summing over the spin states, this can be reduced to

$$\sum |\mathcal{M}|^2 = \frac{2^{14}G_F^4 M_W^4}{(\hat{s} - M_W^2)^2 + M_W^2\Gamma_W^2} (\nu_L \cdot d L \cdot u L \cdot \nu_e \bar{\nu}_L \cdot e - \frac{1}{2} m_L^2 \nu_L \cdot d \nu_e \cdot u \bar{\nu}_L \cdot e) \left[\frac{s_{e\nu}}{M_W^2} - 1 \right]^{-2} \frac{\pi}{m_L\Gamma_L} \delta(p_L^2 - m_L^2), \quad (12)$$

where the particle labels are used to denote their four-momenta. The initial spin and color averages give an additional factor of $\frac{1}{12}$. We neglect the quark and electron masses.

Contrary to what we might expect, we shall see that we cannot make the approximation $\hat{s} = M_W^2$ in calculating the $W \rightarrow e\nu$ background. The off-mass-shell effects of the W are important in kinematic regions where the cross section is small. We multiply the cross section by a QCD-motivated correction factor $K=2$ in the fusion subprocess. The resulting cross section for W^\pm production with $e^\pm\nu$ decay, summed over both charges, is

$$\sigma(\bar{p}p \rightarrow W^\pm \rightarrow e^\pm\nu) = 0.56 \text{ nb} \quad (13)$$

which is in accord with the observed cross section.²

In Fig. 2 we show the electron distributions transverse to the $\bar{p}p$ beam direction, with relative normalization given by Eq. (10). The smearing due to the transverse motion of the produced W is included according to the approximate formula

$$\frac{d\sigma}{dp_T^2} \propto \exp(-25p_T/\sqrt{\hat{s}}), \quad (14)$$

which represents the calculations of Ref. 8. The distributions arising from heavy-lepton decay are shown for various lepton-mass values m_L . The curve for the direct $W \rightarrow e\nu$ decay continues to rise with increasing p_{eT} to the

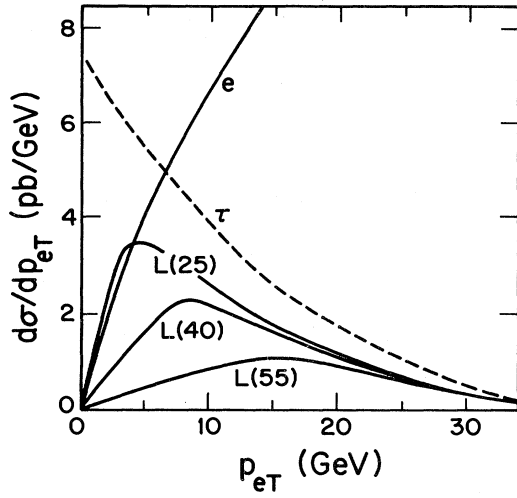


FIG. 2. The momentum distribution of the electron transverse to the beam axis for $\bar{p}p \rightarrow W \rightarrow e$ at $\sqrt{s} = 540$ GeV. The curves labeled e , τ , and L correspond to the decay modes (4), (5), and (3), respectively. The distributions labeled $L(m_L)$ correspond to assuming three different values of the heavy-lepton mass: $m_L = 25, 40,$ and 55 GeV. The e curve, corresponding to the direct $W \rightarrow e\nu$ decay, rises to a Jacobian peak at $p_{eT} \simeq \frac{1}{2}M_W$; we take $M_W = 81$ GeV. The normalization is chosen so that the total cross section for process (4) is $\sigma(\bar{p}p \rightarrow W^\pm \rightarrow e\nu) = 0.56$ nb.

Jacobian peak at $p_{eT} \simeq \frac{1}{2}M_W \simeq 40$ GeV which played a valuable role in the discovery of the W boson.²

From Fig. 1 we see that the L -initiated p_{eT} distribution is masked by the direct $W \rightarrow e$ and $W \rightarrow \tau \rightarrow e$ decays. However, we can unravel these distributions and study the angular spread of the emitted e^+ 's. The angular distributions are shown in Fig. 3, for various intervals of p_{eT} , for each of the three decay modes of the W^+ boson. Inspection of the results shows that to optimize the L signal-to-background ratio we should choose the interval $8 < p_{eT} < 16$ GeV. The comparison is made in Fig. 4. However, before embarking on a detailed discussion of the leptonic decay signature of the L and of other possible

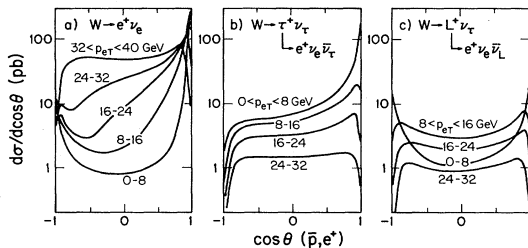


FIG. 3. The angular distributions of the emitted e^+ for various intervals of p_{eT} for (a) $\bar{p}p \rightarrow W^+ \rightarrow e^+$, (b) $\bar{p}p \rightarrow W^+ \rightarrow \tau^+ \rightarrow e^+$, and (c) $\bar{p}p \rightarrow W^+ \rightarrow L^+ \rightarrow e^+$ with $m_L = 40$ GeV. θ is the angle between the incident \bar{p} and the outgoing e^+ in the $\bar{p}p$ center-of-mass frame, $\sqrt{s} = 540$ GeV. The normalization is as for Fig. 2.

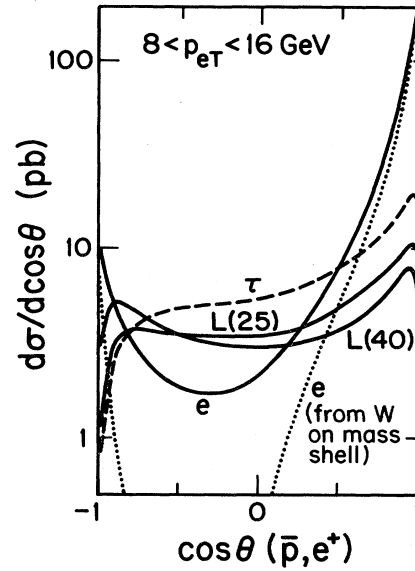


FIG. 4. The e^+ angular distribution for the interval $8 < p_{eT} < 16$ GeV. We show the results for $m_L = 25$ and 40 GeV. The dotted curve represents the W -mass-shell approximation to the $W \rightarrow e\nu$ cross section.

background contributions, it is useful to gain some physical insight into the distributions displayed in Fig. 3.

The angular distribution of an L^+ lepton, produced by the process $\bar{d}u \rightarrow L^+ \nu_L$, has the characteristic asymmetrical form

$$v_L \bar{d} \cdot L \cdot u \propto (1 + \cos \hat{\theta})(1 + v_L \cos \hat{\theta}), \quad (15)$$

where v_L is the L^+ velocity in units of c and $\hat{\theta}$ is the angle between the L^+ and the incident \bar{d} quark in the $\bar{d}u$ center-of-mass frame. In the limit $m_L^2/M_W^2 \rightarrow 0$ (that is, $v_L \rightarrow 1$) the lepton L^+ is produced in a state of positive helicity, whereas for a massive lepton both positive and negative helicity states are populated. Equation (12) incorporates all the effects of this polarization on the L decay distribution.

From Fig. 3 we see that for the direct $W^+ \rightarrow e^+ \nu$ decay the e^+ angular distribution is sharply peaked in the forward direction, relative to the \bar{p} beam, for the relevant range 8 to 16 GeV of p_{eT} , essentially arising from Eq. (15) boosted from the $\bar{d}u$ to the $\bar{p}p$ center-of-mass frame. Only as p_{eT} approaches $\frac{1}{2}M_W$ (i.e., $\hat{\theta} \rightarrow \pi/2$) does the asymmetry disappear. On the other hand, for the τ^+ and L^+ , the sequential decays weaken the e^+ asymmetry, the more so the more massive the L^+ .

An interesting feature of the distributions shown in Fig. 3(a) is that the off-mass-shell effects of the W must be included, as in Eq. (12), to obtain the correct structure of the valleys in the cross section which occur for $p_{eT} \lesssim 25$ GeV. The contributions in the dip region arise from virtual W 's at $\bar{d}u$ center-of-mass energies $\sqrt{\hat{s}}$ far below M_W . Even though the far-off-shell amplitude is suppressed, there is a compensating feature in that the main contribution to the angular distribution occurs for $p_{eT} = \frac{1}{2}\sqrt{\hat{s}}$ and has no dip. This is well illustrated in Fig.

TABLE I. The cross sections for $W^+ \rightarrow e^+$, $W^+ \rightarrow \tau^+ \rightarrow e^+$, and $W^+ \rightarrow L^+ \rightarrow e^+$ for given $(p_{eT}, \cos\theta)$ intervals of the outgoing e , and for different mass values m_L (in GeV) of the heavy lepton L . The normalization corresponds to $\sigma(\bar{p}p \rightarrow W^\pm \rightarrow e^\pm) = 0.56$ nb.

p_{eT} (GeV)	Interval $\cos\theta$	Partial cross section σ (pb)				
		e	τ	L $m_L =$ 25 40 55		
(8,16)	(-0.9,0.2)	2.5	5.3	3.7	3.8	1.8
(10,15)	(-0.9,0.2)	1.5	3.3	2.2	2.3	1.2
(15,20)	(-0.8,-0.2)	1.0	1.4	0.9	0.9	0.8

4 by comparing the true distribution with the direct $W \rightarrow e\nu$ distribution calculated assuming the W remains on shell, $\sqrt{\hat{s}} = M_W$ (the dashed curve).

Finally, we note that the e^- distributions from W^- decays are obtained from the $W^+ \rightarrow e^+$ distributions by the substitution $e^-(\theta) = e^+(\pi - \theta)$.

III. THE L LEPTONIC-DECAY SIGNATURE

In Fig. 4 we selected the p_{eT} interval of the emitted e^+ to maximize the L signal relative to the background. This "window" in p_{eT} is the best that can be done; for larger values of p_{eT} the direct $W \rightarrow e\nu$ events will dominate a possible L signal, and for smaller p_{eT} there are many more τ -initiated events. We see that the optimum angular interval corresponds to $-0.9 < \cos\theta < 0.2$, where θ is the angle between the emitted e^+ and the incident \bar{p} beam. The cross sections $\Delta\sigma$ for this interval are given in Table I for various lepton masses. For example, for a heavy lepton L^+ of mass $m_L = 40$ GeV

$$\Delta\sigma(L) = 3.8 \text{ pb},$$

$$\Delta\sigma(\text{background}) = 7.8 \text{ pb}.$$

Thus to identify such an L signal, at the 3-standard-deviation level, requires a data sample with more than 10^3 $W \rightarrow e^+\nu$ events.

However, there is another background to take into account. Namely, e^+ s emitted from semileptonic decays of heavy quarks (c, b, t) which are pair produced in $\bar{p}p$ collisions. For example, consider

$$\bar{p}p \rightarrow \bar{b}bX \text{ with } \bar{b} \rightarrow \bar{c}e^+\nu_e. \quad (16)$$

A QCD fusion calculation⁹ gives a contribution in the $8 < p_{eT} < 16$ GeV interval some two orders of magnitude above the L signal. The calculation corresponds to a total $\bar{b}b$ production cross section of $5.6 \mu\text{b}$ ($m_b = 4.6$ GeV), assumes a semileptonic branching fraction of 10% and includes a b quark fragmentation function (see Sec. IV). The $\bar{b}b$ background falls off rapidly with increasing p_{eT} as shown in Fig. 5.

To eliminate $\bar{b}b$ and $\bar{c}c$ events we note that the decay electron is accompanied by hadronic debris from the quark cascade decays [for example, the b and \bar{c} decays of Eq. (16)]. One way to suppress this background is to impose cuts on the accompanying hadronic p_T . For example, we find that the heavy-quark background can be

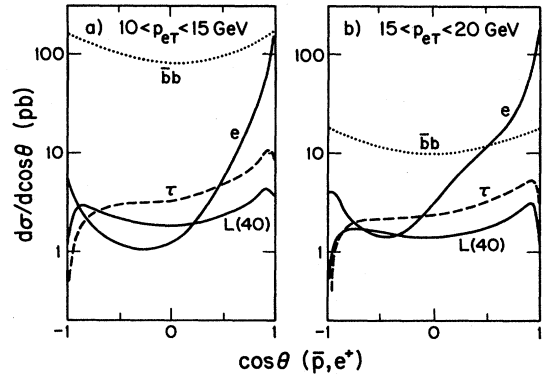


FIG. 5. The e^+ angular distributions for a heavy lepton of mass 40 GeV, together with background contributions, for two intervals of p_{eT} . The effect of the $\sum p_T < 10$ GeV cut on the debris reduces the $\bar{b}b$ and $\bar{c}c$ backgrounds to well below the signal.

essentially eliminated by rejecting events with hadronic $\sum_i |\vec{p}_{iT}| > 10$ GeV.

We conclude that the detection of a heavy lepton L via the observation of its decay electron requires a $\bar{p}p$ collider experiment with an integrated luminosity in excess of 1000 nb^{-1} . If the mass is in the range $20 < m_L < 50$ GeV, then, in the optimum interval of p_{eT} and θ , the $W \rightarrow L \rightarrow e$ signal is at the 3–4 pb level. Even then the background due to $W \rightarrow \tau \rightarrow e$ and $W \rightarrow e$ exceeds the signal. The proposed introduction of a microvertex detector in the UA1 experiment should help suppress the τ (and also the $\bar{b}b$) background by separating its production and decay vertices in these events.

IV. HADRONIC-DECAY SIGNATURE OF THE L

We have proposed⁵ that the hadronic decay mode of the L serves as the best signature of a new heavy lepton at the $\bar{p}p$ collider. The relevant decay chains are

$$W \rightarrow L\nu_L \rightarrow u\bar{d}\bar{\nu}_L\nu_L \text{ or } c\bar{s}\bar{\nu}_L\nu_L. \quad (17)$$

Color enhances these decays so that the sum of the two rates is

$$\sigma(W \rightarrow L\nu \rightarrow Q\bar{q}\bar{\nu}\nu) = \frac{6}{9} \left(1 - \frac{3}{2}r + \frac{1}{2}r^3\right) \sigma(W \rightarrow e\nu) \quad (18)$$

with $r = m_L^2/M_W^2$ [compare Eq. (10)]. Since now we have an energetic primary-decay neutrino with only one secondary-decay neutrino, these events have, on the average, much larger missing momentum than in the leptonic decays of the L . We therefore have a distinctive signature for the L of high missing transverse momentum (due to $\bar{\nu}_L\nu_L$) balanced by two (possibly overlapping) quark jets. The calculation of the rate proceeds as for the leptonic decay, with the amplitude for

$$\bar{d}u \rightarrow W^+ \rightarrow L^+\nu_L \rightarrow (Q\bar{q}\bar{\nu}_L)\nu_L \quad (19)$$

given by Eq. (11) with $e^+ \rightarrow \bar{q}$ and $\nu_e \rightarrow Q$. The missing-transverse-momentum distribution for a lepton of mass $m_L = 40$ GeV is shown in Fig. 6.

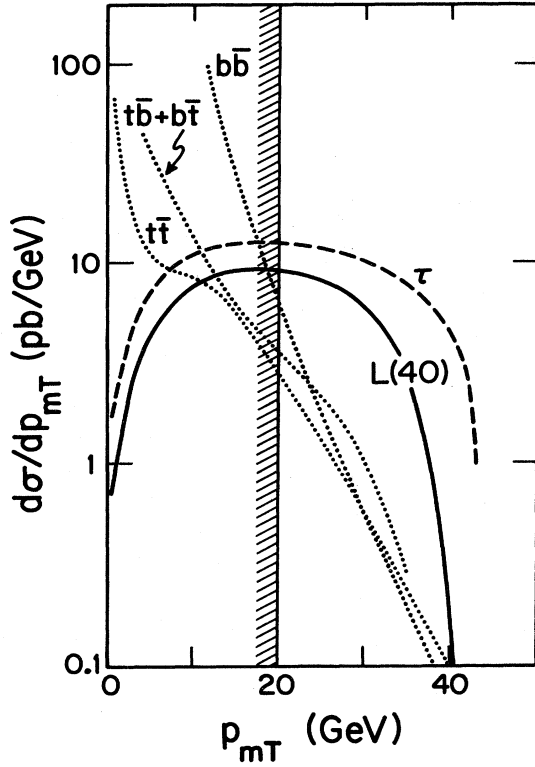


FIG. 6. The missing transverse momentum (p_{mT}) distributions arising from $W \rightarrow L\nu_L \rightarrow \bar{q}Q\bar{\nu}_L\nu_L$ with $m_L = 40$ GeV and $L = \tau$, taking a $\tau \rightarrow$ hadrons branching fraction of 65%. The normalization is as in Fig. 2, and we sum over W^\pm -initiated events. The curves which rapidly decrease with increasing p_{mT} are background contributions coming from the production and subsequent semileptonic decay of heavy quarks.

We also show in Fig. 6 possible background contributions from sequential τ decay

$$W \rightarrow \tau\nu_\tau \rightarrow u\bar{d}\bar{\nu}_\tau\nu_\tau \quad (20)$$

and from heavy-quark production with one or more subsequent semileptonic decays. We estimate heavy-quark hadroproduction from the lowest-order QCD processes $q\bar{q}, gg \rightarrow c\bar{c}, b\bar{b}, t\bar{t}$ (ignoring the possibility of flavor excitation¹⁰ and nonperturbative diffractive production). We assume a top quark of mass 35 GeV. We allow for the full cascade decay of the heavy quarks and assume that the charged leptons from the semileptonic decays are identified if, and only if, $p_{eT} > 10$ GeV and $p_{\mu T} > 4$ GeV. We take 10% branching fractions for each semileptonic decay mode, except for τ decay where we take 17%. The heavy quarks are assumed to fragment into heavy spinless or unpolarized hadrons, of the same masses as the quarks. We include a fragmentation probability distribution of the form¹¹

$$D(z) = \text{constant} / \{z[1 - 1/z - \epsilon/(1-z)]^2\}, \quad (21)$$

where z is the hadron/quark c.m. momentum fraction and $\epsilon = 0.15(m_c^2/m_Q^2)$ which is consistent with c and b production data.

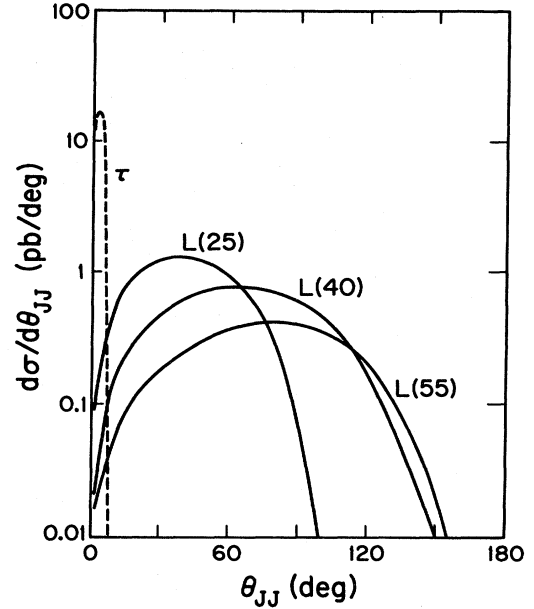


FIG. 7. The distribution of the opening angle θ_{JJ} , as seen in the $\bar{p}p$ frame, between the two jets emerging from $\bar{p}p \rightarrow W \rightarrow L\nu_L \rightarrow JJ\bar{\nu}_L\nu_L$, for different masses of the heavy lepton L . The cuts to remove the background events have been imposed.

We see from Fig. 6 that the p_{mT} distribution arising from heavy-quark production falls off rapidly with increasing p_{mT} , and that for $p_{mT} \geq 20$ GeV/ c the distribution comes mainly from L - and τ -initiated events. This is just the region where it should be feasible to experimental-

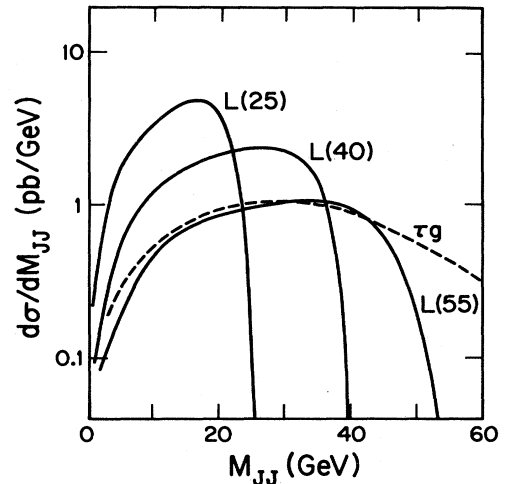


FIG. 8. The invariant-mass (M_{JJ}) distribution of the two jets arising from $W \rightarrow L\nu_L \rightarrow JJ\bar{\nu}_L\nu_L$ for different masses of the heavy lepton L . The cuts to remove the background events have been imposed. The dashed curve is the possible remaining background contribution from $Wg \rightarrow \tau\nu_\tau g \rightarrow (\bar{d}u)\bar{\nu}_\tau\nu_\tau g$ with $p_{gT} > 8$ GeV and $K=2$. The normalization is as in Fig. 2 and we sum over W -initiated events.

ly measure p_{mT} reliably.

For the heavy-quark events the decay neutrino (or neutrinos) will be accompanied by other decay debris, whereas for the $W \rightarrow L \nu_L$ signal the primary neutrino is unaccompanied. Thus, in a similar way to before, we can suppress the heavy-quark background by imposing an isolation cut on the missing transverse momentum. Subsequently we require that $\sum |\vec{p}_T| < 5$ GeV, where the sum is over all fragments within 20° of the p_{mT} direction in the transverse plane. We find that this cut suppresses the heavy-quark background by an order of magnitude or more.

The two quark jets emerging from the decay of the heavy lepton, shown in Eq. (19), are quite energetic and should be recognizable. For the results we present below we impose the requirement that $p_T(\text{jet}) > 8$ GeV/c for both jets (together with the $p_{mT} > 20$ GeV and the isolation cut). In Fig. 7 we show the prediction for the opening angle in the $\bar{p}p$ center-of-mass frame between the two jets for different masses of the parent lepton. The invariant-mass (M_{JJ}) distribution of the two jets is shown in Fig. 8, again for various lepton masses. This M_{JJ} distribution offers an excellent signature for $W \rightarrow L \nu_L$ events. The upper end point of the distribution is a good indicator of the mass of the new lepton. Moreover, the total event rate is healthy. After imposing all the cuts, the integrated heavy-lepton signal relative to the total $W^\pm \rightarrow e \nu$ rate is

$$\frac{\sigma(W \rightarrow L \nu \rightarrow JJ \bar{\nu} \nu)}{\sigma(W \rightarrow e \nu)} = \begin{cases} 0.13 & \text{for } m_L = 25 \text{ GeV} , \\ 0.11 & \text{for } m_L = 40 \text{ GeV} , \\ 0.08 & \text{for } m_L = 50 \text{ GeV} , \\ 0.05 & \text{for } m_L = 60 \text{ GeV} . \end{cases} \quad (22)$$

$$|\mathcal{M}|^2 = \left[\frac{1}{12} \right] \frac{2^{12} \pi \alpha_s G_F^2 M_W^6}{3 \hat{u} \hat{t}} \left[-\tau \cdot \bar{d} \nu_\tau \cdot \bar{d} - \tau \cdot u \nu_\tau \cdot u + \frac{1}{2} (\hat{u} + \hat{s}) \nu_\tau \cdot \bar{d} + \frac{1}{2} (\hat{t} + \hat{s}) \tau \cdot u \right] \frac{\pi}{M_W \Gamma_W} \delta(W^2 - M_W^2) , \quad (25)$$

where the particle names are used to denote their four-momenta, $\hat{s}, \hat{t}, \hat{u}$ refer to the subprocess $\bar{d}u \rightarrow Wg$, and the fermions are taken to be massless. Ignoring τ -spin correlations, we multiply by the τ -decay factor

$$B_\tau d\Gamma_\tau / \Gamma ,$$

where $d\Gamma_\tau \propto \tau \cdot Q \bar{\nu}_\tau \cdot \bar{q}$ and B_τ is the $\tau \rightarrow Q \bar{q} \bar{\nu}_\tau$ branching fraction, and then integrate over the phase space of all final-state particles. With the cut $|\vec{p}_{WT}| > 8$ GeV/c we find, with $K=2$,

$$\sigma(\bar{p}p \rightarrow W^\pm g \rightarrow \tau \nu_\tau g) = 0.068 \text{ nb} . \quad (26)$$

The contributions from the crossed subprocesses $qg \rightarrow W^\pm q$ and $\bar{q}g \rightarrow W^\pm \bar{q}$ were found to give a much smaller contribution. Constructing M_{JJ} from the ($\bar{q}Q$) and g jets gives the τ background curve shown on Fig. 8. This is an upper estimate of this background since the τ may often be distinguished as a single particle jet.

That is, for a wide range of the mass of the lepton the event rate is about 10% of the W signal.

It remains to eliminate the background from τ -initiated events

$$W \rightarrow \tau \nu_\tau \rightarrow u \bar{d} \bar{\nu}_\tau \nu_\tau .$$

From Fig. 6 we see that the τ signal is comparable to the L signal. However, for the hadronic decay modes we do not have the same difficulty in distinguishing between L and τ decays that we had for the leptonic modes. The $u\bar{d}$ system from τ decay will be observed as a single narrow, energetic jet [with typically $20 < p(\text{jet}) < 40$ GeV/c] of low multiplicity, and should be readily recognizable. Moreover, the τ -initiated events will populate the $M_{JJ} < m_\tau$ region of the M_{JJ} plot and so, in principle, should give no background to the L distributions.

However, there is one part of the τ signal that may cause confusion. In a fraction of events the W will be produced at large p_T (say, $p_{WT} > 8$ GeV/c) recoiling against a visible parton jet, namely, via

$$\bar{q}Q \rightarrow Wg \rightarrow \tau \nu g \quad (23)$$

or the crossed QCD processes. Thus in the construction of M_{JJ} we may be misled into taking the ($u\bar{d}$) jet from τ decay together with the gluon jet. For these events the τ signal will be smeared over a wide range of M_{JJ} . To calculate this background we use lowest-order QCD. The spin- and color-averaged matrix element squared for $\tau \nu_\tau g$ production

$$\bar{d}u \rightarrow W^+ g \rightarrow \tau^+ \nu_\tau g \quad (24)$$

is given by

V. CONCLUSION

We have studied ways of using the $W \rightarrow L \nu_L$ decay mode to detect new heavy leptons at the $\bar{p}p$ collider. We investigated signatures arising from both leptonic and hadronic decays of the L . The former, based on observing high- p_T electrons emitted from $L \rightarrow e \nu_e \bar{\nu}_L$, is plagued by backgrounds from both the direct $W \rightarrow e \nu_e$ decay and the sequential $W \rightarrow \tau \nu_\tau \rightarrow e \nu_e \bar{\nu}_\tau \nu_\tau$ decay. The signal, which integrated over the optimum kinematic range of the emitted electron is about 4 pb, is never above the background.

On the other hand, the hadronic-decay signature of the L is much more promising. The events have the distinctive signal of a large missing transverse momentum balanced by two reasonably energetic jets. After selective cuts have been applied to remove background contributions, the event rate is about 10% of that for $W^\pm \rightarrow e \nu$, provided the mass of the new lepton is in the range 20 to 50 GeV.

After this paper was submitted for publication, we received a paper by Gottlieb and Weiler¹² which makes analytic evaluations of $W \rightarrow L \rightarrow e$ decay distributions.

ACKNOWLEDGMENTS

This research was supported in part by the University of Wisconsin Research Committee with funds granted by

the Wisconsin Alumni Research Foundation, and in part by the Department of Energy under Contract No. DE-AC02-76ER00881.

-
- ¹W. Bartel *et al.*, Phys. Lett. 123B, 353 (1983); R. Brandelik *et al.*, *ibid.* 99B, 163 (1981); C. H. Berger *et al.*, *ibid.* 99B, 489 (1981); D. P. Barber *et al.*, Phys. Rev. Lett. 45, 1904 (1980).
- ²UA1 collaboration, G. Arnison *et al.*, Phys. Lett. 122B, 103; 126B, 398 (1983); 129B, 273 (1983); UA2 collaboration, M. Banner *et al.*, *ibid.* 122B, 476; P. Bagnara *et al.*, *ibid.* 129B, 130 (1983).
- ³D. Cline and C. Rubbia, Phys. Lett. 127B, 277 (1983); D. Cline, Moriond conference report, 1983 (unpublished).
- ⁴S. Weinberg, Phys. Rev. Lett. 50, 387 (1983); R. A. Arnowitt, A. H. Chamseddine, and Pran Nath, *ibid.* 50, 232 (1983); Phys. Lett. 129B, 445 (1983); D. A. Dicus, S. Nandi, and X. Tata, *ibid.* 129B, 451 (1983); D. A. Dicus, S. Nandi, W. W. Repko, and X. Tata, Austin Report No. 521, 1983 (unpublished); V. Barger, R. W. Robinett, W. Y. Keung, and R. J. N. Phillips, Phys. Lett. 131B, 372 (1983); Phys. Rev. D 28, 2192 (1983).
- ⁵V. Barger, H. Baer, A. D. Martin, E. W. N. Glover, and R. J. N. Phillips, Phys. Lett. 133B, 449 (1983).
- ⁶J. F. Owens and E. Reya, Phys. Rev. D 17, 3003 (1978).
- ⁷M. Glück, E. Hoffman, and E. Reya, Z. Phys. C 13, 119 (1982).
- ⁸F. Halzen, A. D. Martin, and D. M. Scott, Phys. Lett. 112B, 160 (1982).
- ⁹V. Barger, A. D. Martin, and R. J. N. Phillips, Phys. Lett. 125B, 339 (1983); 125B, 343 (1983); Phys. Rev. D 28, 145 (1983); V. Barger, H. Baer, A. D. Martin, and R. J. N. Phillips, *ibid.* 29, 887 (1984).
- ¹⁰B. L. Combridge, Nucl. Phys. B151, 429 (1979); V. Barger, F. Halzen, and W. Y. Keung, Phys. Rev. D 24, 1428 (1981); R. Odorico, Phys. Lett. 118B, 425 (1982).
- ¹¹C. Peterson, D. Schlatter, I. Schmitt, and P. M. Zerwas, Phys. Rev. D 27, 105 (1983).
- ¹²S. Gottlieb and T. Weiler, Phys. Rev. D 29, 2005 (1984).